

Communication

Polymer-Based High Diffraction Efficiency and High Resolution Volume Holographic Transmission Gratings

Riccardo Castagna^{1,2,*}, Andrea Di Donato³, Oriano Francescangeli⁴ and Daniele Eugenio Lucchetta^{4,5,*}¹ URT-CNR, Università di Camerino (UNICAM), Polo di Chimica, Via Sant'Agostino, 1, 62032 Camerino, Italy² CNR, Institute of Heritage Science, Via Madonna del Piano, 10, 50019 Sesto Fiorentino, Italy³ Dip. di Ingegneria dell'Informazione, Università Politecnica delle Marche, Via Brecce Bianche, 60131 Ancona, Italy⁴ Dip. di Scienze e Ingegneria della Materia, dell'Ambiente ed Urbanistica (SIMAU), Università Politecnica delle Marche, Via Brecce Bianche, 60131 Ancona, Italy⁵ Optoacoustic Lab, Dip. di Scienze e Ingegneria della Materia, dell'Ambiente ed Urbanistica (SIMAU), Università Politecnica delle Marche, Via Brecce Bianche, 60131 Ancona, Italy

* Correspondence: riccardo.castagna@cnr.it (R.C.); d.e.lucchetta@univpm.it (D.E.L.)

Abstract: We report on the optical characterization of very high-efficiency and high-resolution holographic volume phase transmission gratings. The gratings are recorded in a new photo-polymerizable mixture made by epoxy-resin and multi-acrylate. The epoxy-resin used is known to make tenacious acrylate-based films. The holographic mixture contains two photo-initiators, the synergic effect of which enables a reliable photo-polymerization process in the visible region of the electromagnetic spectrum. The recorded holograms are mechanically stable, show long-term temporal stability and very high values of diffraction efficiency, coupled with good angular selectivity due to a relatively narrow band of wavelengths. We measured the intensity of the transmitted beam and calculated the intensity of the diffracted beam at different wavelengths, deriving the refractive index modulation and the grating pitch by fitting the experimental data with a slightly modified theoretical approach. These kind of mixtures can be used in several fields of application, such as chemical or bio-sensors, high resolution optical sensors, high-density optical data storage, encryption and security.

Keywords: holographic sensors; gratings; polymers; data storage; security; acrylate; epoxy resins



Citation: Castagna, R.; Di Donato, A.; Francescangeli, O.; Lucchetta, D.E. Polymer-Based High Diffraction Efficiency and High Resolution Volume Holographic Transmission Gratings. *Chemosensors* **2022**, *10*, 356. <https://doi.org/10.3390/chemosensors10090356>

Academic Editor: Ali Othman

Received: 5 August 2022

Accepted: 29 August 2022

Published: 1 September 2022

Publisher's Note: MDPI stays neutral with regard to jurisdictional claims in published maps and institutional affiliations.



Copyright: © 2022 by the authors. Licensee MDPI, Basel, Switzerland. This article is an open access article distributed under the terms and conditions of the Creative Commons Attribution (CC BY) license (<https://creativecommons.org/licenses/by/4.0/>).

1. Introduction

Holographic biosensors and chemical sensors are technologies requiring the continuous development of novel materials. Nowadays, there is a large variety of different materials available that can be used to fabricate holograms to be used as sensors [1–9]. Azobenzene and thiolene polymers play an important role in the field [10–12]. In addition, multi-acrylate molecules are very useful for recording and retrieving information regarding the physical parameters characterizing the impinging polymerizing light [13–15]. They form the basis of holographic polymer-dispersed liquid crystals (HPDLCs) that are organic mixtures widely used to record transmission and reflection holograms [16–23]. Under irradiation, these materials show significant changes in their optical properties, such as changes in the average refractive index and in refractive index modulation, and in their mechanical properties, such as patterning of the surface or volume. These changes can be used to store and retrieve information in the surface or in the bulk of the used samples, in single or multi-layered solutions [24–27]. Usually, in the blue wavelength range, high recording sensitivity, high spatial resolution (>7000 lines/mm) [17], easy processability, high optical quality over large areas or volumes [28] and, finally, low shrinkage (a useful feature for large scale industrial applications) can be achieved. Two possible configurations (geometries) are most often used to detect changes in the optical or mechanical properties of the recorded holograms: the transmission geometry and the reflection geometry. When a

light beam impinges on the recorded hologram, the diffracted beam can be found in the space region behind the sample (if the operation is in transmission mode) or in the space region in front of the sample (if the operation is in reflection mode). The transmission mode is often used in free space configurations in which the “reading” of the sensor optical properties can be carried out even at high distance [29]; in contrast, the reflection mode is often used in optical fibers and guided configurations [30,31]. In the latter case, the core material of the optical fiber is responsible for the changes in the refractive index modulation due to interaction with the chemical or biological species surrounding the core itself. In this paper, we focus on a holographic mixture in which high efficiency transmission and reflection holograms can be recorded. This combination was originally developed to be used in two important fields of application: high density optical storage, to replace liquid crystals in HDPLCs mixtures to overcome their drawbacks, and photomobile polymer films, the motion of which is induced and controlled by light [17,20,23,32,33]. To make the system more versatile, we slightly modify the original recipe to improve some physical parameters that can be useful in the field of sensor development. We perform a first optimization of the mixture using a two photo-initiator system to make it more sensitive to the writing wavelength that, in our case, is $\lambda = 457.9$ nm. We then record holographic transmission phase gratings with different pitches, in the range of 170–200 nm, to determine the relationship between the recording conditions and measured values of diffraction efficiency. We also measure the physical parameters characterizing the optical properties of the written gratings (i.e., diffraction efficiency, refractive index modulation and grating pitch) using an original experimental approach in which a large band white light impinges on the recorded grating at different angles. From a theoretical point of view, the values of the optical parameters are determined by fitting the experimental data with a slightly modified theoretical approach firstly given by Kogelnik [34,35].

2. Materials and Methods

2.1. Materials

Tris(4-hydroxyphenyl) methane triglycidyl ether (THPMTGE), dipentaerythritol-mono-hydroxy-penta-acrylate (DPMHPA), 2,6-Bornanedione (BD) were obtained from Merck; bisacylphosphine oxide (BAPO) was obtained from Ciba Specialty. The chemical formulae of the compounds used are reported in Figure 1.

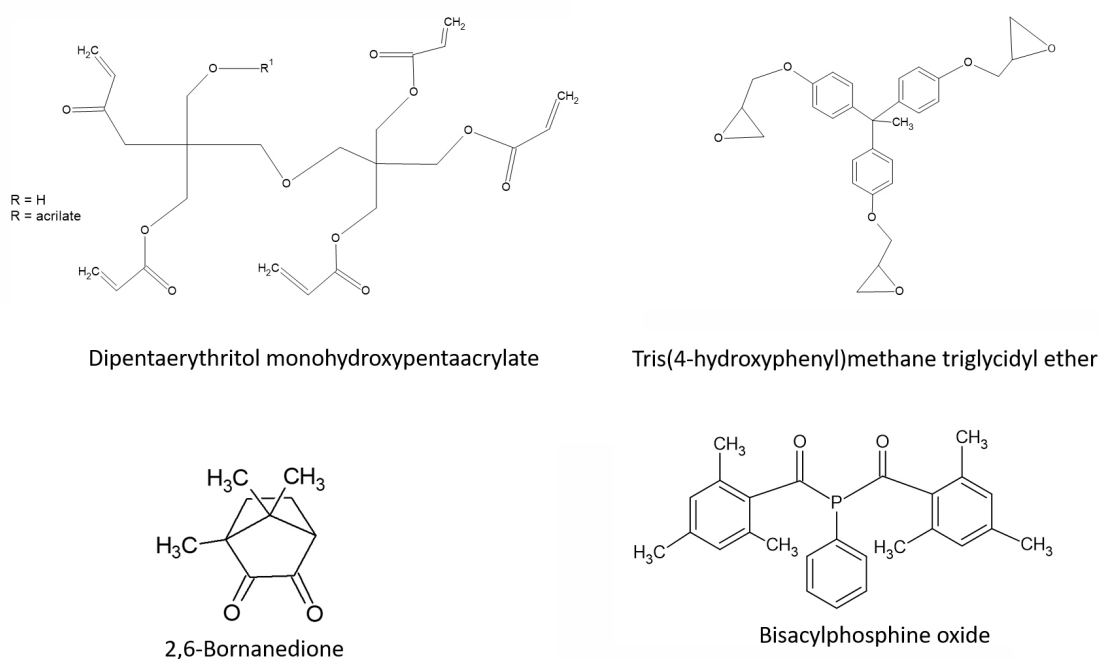


Figure 1. Chemical structures of the used compounds.

2.2. Methods

BD and BAPO were first added to DPHMPA and the mixture was stirred for ≈ 3 h in the dark at room temperature. At the same time, aromatic epoxy resin THPMTGE was kept at 80°C for 15 min. In this condition, THPMTGE has low viscosity and is easy to handle. At this stage, it was mixed together with DPMHPA containing the two photo-initiators (PIs) and the mixture was stirred for at least 3 h until a pale yellow syrup was obtained. The final concentrations of the components of the holographic mixture were: DPHMPA 68% (w/w); THPMTGE 28%; BD 2%; BAPO 2%.

2.3. Holographic Set-Up

We created the cells using a sandwich-like configuration comprising two microscope glasses separated by two $100\ \mu\text{m}$ thick Mylar stripes. The cell was heated at $\approx 60^\circ\text{C}$ to allow the filling of the cell by capillary action. The sample was then irradiated by two interfering CW DPSS s-polarized laser beams at $\lambda = 457.9\ \text{nm}$ (see Figure 2). The writing power used was $P = 100\ \text{mW}$ per beam. The spot region had a diameter d of $\approx 5\ \text{mm}$. Typical recording angles θ were in the range 30° to 60° . The light emitted by the DPSS laser passed through an attenuation system made by a half-wave ($\lambda/2$) plate and a linear Glan–Thompson polarizer (P). By rotating the plate, the intensity of the laser could be controlled with great accuracy. A mirror deflected the light towards a beam expander (BE) with a $2\times$ magnification factor. The magnified beam passed through a 50% beam splitter and the resulting two beams were redirected by two mirrors onto the sample. A low power He-Ne laser positioned at the Bragg diffraction angle was used to detect the grating formation. After a few seconds, the diffracted signal appeared. To ensure a complete photo-polymerization of the spot area, the total irradiation time was set at 5 min. During the photo-polymerization, a phase-separation process occurred between the polymerized and non-polymerized parts of the starting monomer mixture. The result was a periodic structure (holographic grating) permanently recorded inside the interfering region of the two beams. A dielectric contrast or refractive index modulation was now present inside the spot region. This modulation could be readily detected using optical techniques, as follows: the sample, placed on a motorized goniometer, was illuminated through an optical fiber connected to an incoherent large band Xe-light source emitting wavelengths in the range of 350–1000 nm. The sample was then rotated and the transmitted signal was captured by a spectrometer connected to a real-time data acquisition system. The spectra of the transmitted light were detected using a real-time spectrometer for each value of the incident angle. Other spectra were simply acquired by illuminating the sample with the same white source and, at the same time, acquiring the transmitted signal with an optical fiber connected to the spectrometer.

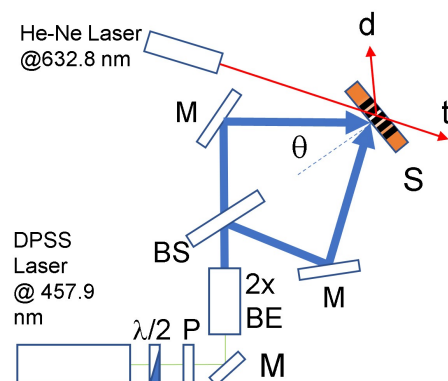


Figure 2. Schematic representation of the writing setup for the high-resolution transmission gratings. $\lambda/2$ = half wavelength plate; P = polarizer; M = mirror; $2 \times \text{BE}$ = $2 \times$ beam expander; BS = beam splitter; S = sample; d and t = diffracted and transmitted beams, respectively. The recorded transmission grating is shown in black.

3. Results and Discussion

In this investigation, we used a composite polymer mixture consisting of a combination of a multi-functional acrylate monomer DPHMPA and an epoxy-aromatic resin THPMTGE. The final mixture is a highly viscous fluid that can be introduced into a glass cell by capillarity, as explained in the Methods section. The high viscosity of the mixture and the absence of any solvent are useful features for applications in which thick polymer films are required [36–38]. The DPHMPA-THPMTGE mixture was photo-sensitized to $\lambda = 457.9$ nm by adding two PIs: (1) BAPO—a very efficient photo-initiator in the UV-A region, yielding carbon-centered and phosphorous-centered free radicals under irradiation, and (2) BD—the maximum absorption of which is at $\lambda \approx 470$ nm. The synergic effect of the used PIs generated an efficient photo-polymerization of DPHMPA [39]. The chemical formulae of the compounds used are reported in Figure 1. In Figure 3, a transmission spectrum written in the holographic mixture THPMTGE/DPHMPA is shown. The corresponding diffraction efficiency is around 85%. The material proposed represents an advance with respect to the previous generation of widely used HPDLCs that are the direct competitors of our mixtures. However, the absence of liquid crystals is a great advantage when seeking sensors that are insensitive to pressure, temperature and electric or magnetic fields. Moreover, the material shows high values of diffraction efficiency (up to 85.0%), low shrinkage [17], low light scattering and high transparency. The absence of liquid crystals should enable more straightforward bio-/chemo-functionalization. With respect to the diffraction efficiency, we detected a negligible reduction in its value from 85.0% to 84.6% over approximately one year. This implies that the optical properties of the recorded structures remain unaltered in this temporal range. According to Kogelnik's theory, the diffraction efficiency of a one-dimensional transmission phase grating can be written as:

$$\eta(\nu, \zeta) = e^{-\frac{\alpha d}{\cos\theta}} \frac{\sin\left(\sqrt{\nu^2 + \zeta^2}\right)^2}{1 + \frac{\zeta^2}{\nu^2}} \quad (1)$$

with coupling and detuning parameters, respectively defined as:

$$\nu = \frac{\pi \times \delta n \times d}{\lambda \times \cos\theta} \quad (2)$$

$$\zeta = \Delta\theta \times \beta \times d \times \sin\theta_0 \quad (3)$$

where δn is the induced refractive index variation, d the grating thickness, λ the reading wavelength in the free space, θ the angle of incidence, θ_0 the Bragg angle, α the distributed absorption coefficient and n the average refractive index of the medium and $\beta = 2\pi n/\lambda$. The parameter $\Delta\theta$ in Equation (3) describes the de-phasing term appearing when λ or θ are varied. The relationship between the wavelength, the angle of incidence and the grating period Λ is described by the following relation:

$$\Delta\theta = \frac{2\pi}{\Lambda} \times \sin\theta - \left(\frac{2\pi}{\Lambda}\right)^2 \frac{\lambda}{4 \times \pi \times n} \quad (4)$$

Under the Bragg condition $\Delta\theta = 0$, the Equation (4) takes the well-known expression:

$$\theta_0(\lambda) = \arcsin\left(\frac{\lambda}{2 \times \Lambda \times n}\right) \quad (5)$$

which leads to a new expression for the diffraction efficiency:

$$\eta(\lambda, \delta n) = e^{-\frac{2\alpha d}{\cos\theta_0(\lambda)}} \sin^2\left(\frac{\pi \times \delta n \times d}{\lambda \cos\theta_0(\lambda)}\right) \quad (6)$$

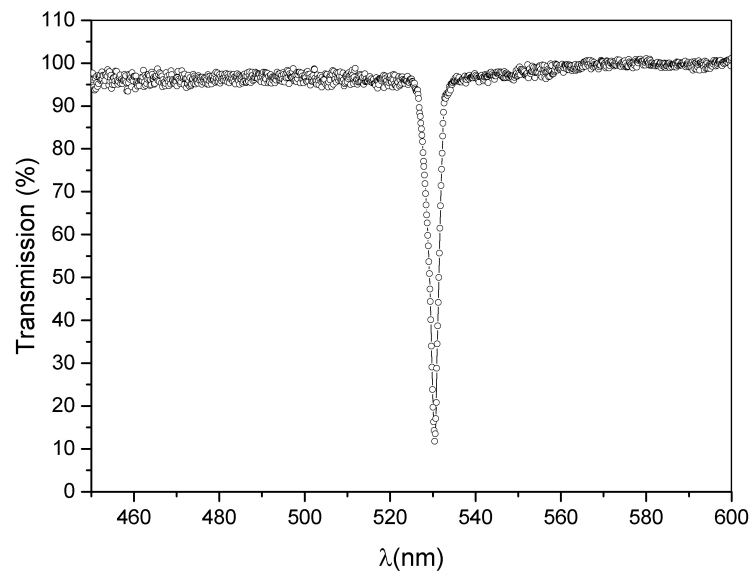


Figure 3. High efficiency transmission spectrum recorded in our holographic mixture. Recording power $P = 100$ mW per beam, $\lambda = 457.9$ nm, grating pitch $\Lambda = 170$ nm.

Figure 4 shows several transmission spectra as a function of the rotation angle (or wavelength). Each rotation angle has a corresponding diffracted narrow range of wavelengths. Each rotation angle corresponds to a Bragg angle for the narrow band of colors selected by the grating and subtracted from the transmitted signal. Each spectrum shows, after proper calibration of the spectrometer, a quite narrow peak centered around the main diffracted wavelength ranges. The height of the peak directly provides the value of the diffraction efficiency of the diffracted signal [40,41]. By measuring the values of the diffraction efficiency for each single peak, we can plot the behavior of the diffraction efficiency of the grating as a function of the wavelength (or the Bragg angles). This behavior is reported in Figure 5.

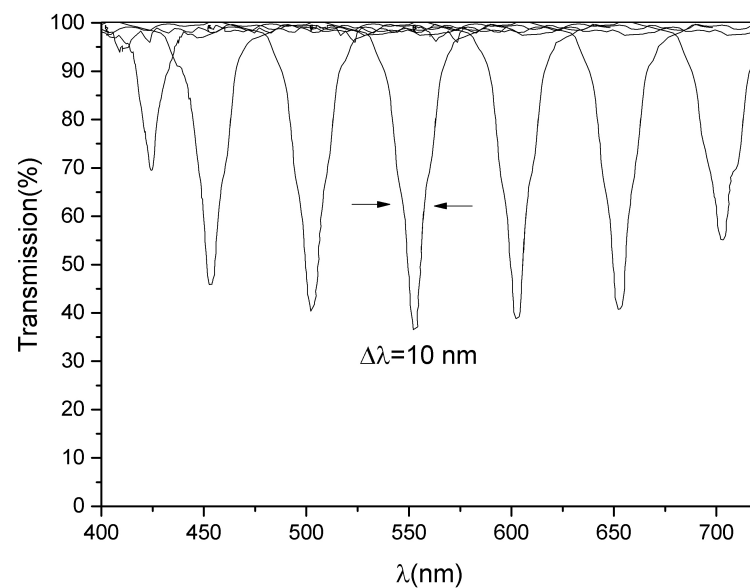


Figure 4. Spectra of a transmission grating taken at different diffraction angles (53.4° , 51.0° , 45.4° , 39.4° , 32.6° , 24.1° , 10.7°). The maximum measured value of diffraction efficiency is $>60\%$ with a FWHM of ≈ 10 nm, grating pitch $\Lambda \approx 230$ nm.

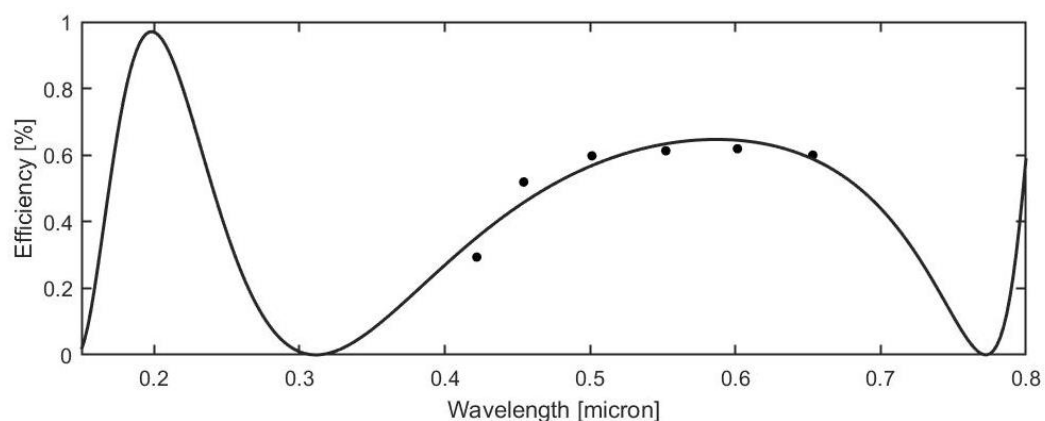


Figure 5. Data fit of the experimental values of the diffraction efficiency as a function of the wavelength.

The data in Figure 5 can be fit using Kogelnik's theory; the agreement between the theoretical expression, reported in Equation (1), and the experimental data is excellent. The fitting procedure enables determination of the grating refractive index modulation $\delta n \sim 2.90 \pm 0.03 \times 10^{-3}$ and the pitch $\Lambda = 233 \pm 10$ nm, assuming an average refractive index $n = 1.52$ and a thickness $d = 100$ μm . The data obtained from the fitting have been corrected for angle- and polarization-dependent Fresnel refraction.

At this stage, certain observations on the photo-polymerization process as the basis of the grating formation should be highlighted.

While BAPO is extremely efficient in the UV-A region, it is less efficient at low concentration in the Vis-region of interest, namely, the visible region of the electromagnetic field in which the photo-polymerization process affects the grating formation ($\lambda = 457.9$ nm). As mentioned, the maximum absorption of BD is at $\approx \lambda = 470$ nm, which is compatible with the chosen wavelength. However, the use of a single photo-initiator under our experimental conditions did not achieve the formation of gratings with appreciable diffraction efficiency. This phenomenon is probably due to the mechanical constrictions of molecular mobility in the holographic sample that requires a more efficient PIs system to promote an optimal photo-polymerization process. The molecules present in the sample were in a static configuration, strongly limiting one or more of the factors at the basis of the reactivity of a chemical system. These factors are: (a) the probability that molecules will meet, (b) the correct activation energy, and (c) the right molecular orientation. The molecular weight of DPHMPA is 524.21, while that of THMPMTGA is 460.52, corresponding to relatively high molecular weights for single molecules (i.e., not inserted in a polymer configuration). They are used in the system to form a high viscous layer, as indicated in the Materials and Methods section. This configuration does not allow the molecules to rotate and/or to move freely in the reaction environment, strongly limiting the possibilities of inter-molecular reactivity in the matrix. In short, to produce efficient polymerization reactions in our system, we can only choose: the PIs in terms of the efficiency of free radical formation and the quantity of multi-functional monomers able to store the information related to the physical properties of the incoming beams. The activation of oxygen- and carbon-centered free radicals on BD and the induction of free radical formation on the BAPO, that efficiently produces carbon- and phosphorous-centered free radicals, injects free radicals that are immediately available for the beginning of the desired photo-polymerization process in the system. With respect to the mechanism of action of BD, the literature reports the formation of carbon- and oxygen-centered free radicals. A possible mechanism involving the triplet state of the molecule is illustrated in Figure 6. However, the two PIs do not affect the THPMTGE polymerization [15,17]. In our system, THPMTGE creates a sort of matrix for the DPHMPA that prevents mechanical shrinkage [17].

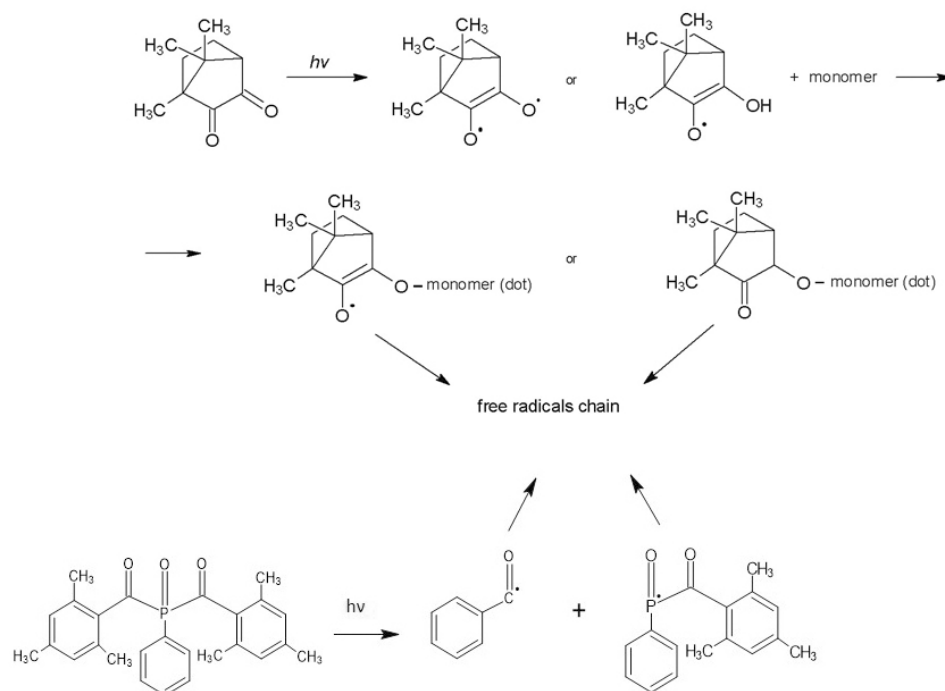


Figure 6. Scheme of the hypothesized mechanism concerning the formation of oxygen-centered free radicals on BD molecule under Vis-irradiation and phosphorous- and carbon-centered free radicals on the BAPO molecule.

4. Conclusions

In this paper, we report the optical characterization of one-dimensional volume transmission gratings recorded in a composite polymer mixture made from epoxide and multifunctional acrylate monomers. The optical parameters characterizing the recorded high-resolution holograms are derived by fitting the experimental data using a slightly modified version of Kogelnik's theory. The experimental approach allows for the direct measurement of the diffraction efficiency of the grating as a function of the wavelength and presents the possibility of measuring certain optical parameters, such as the refractive index modulation and the grating pitch. The stability of the recorded holograms and their optical properties represent promising results for their application in different research fields, ranging from holographic bio- and chemical sensors to optical data storage and data encryption/security.

Author Contributions: Conceptualization, R.C., D.E.L.; methodology, R.C., D.E.L.; software, A.D.D.; validation, R.C., D.E.L.; formal analysis, A.D.D.; investigation, R.C., D.E.L.; resources, R.C.; writing—original draft preparation, R.C., D.E.L.; writing—review and editing, D.E.L., R.C., A.D.D., O.F.; supervision, O.F.; project administration, R.C.; funding acquisition, R.C., D.E.L. All authors have read and agreed to the published version of the manuscript.

Funding: R.C. thanks “Marche Applied Research Laboratory for Innovative Composites” (MARLIC), POR Marche FESR 2014–2020, Regione Marche (Italy).

Institutional Review Board Statement: Not applicable.

Informed Consent Statement: Not applicable.

Data Availability Statement: Data are available from the authors under reasonable request.

Acknowledgments: R.C. acknowledge the support of “Marche Applied Research Laboratory for Innovative Composites” (MARLIC), POR Marche FESR 2014–2020, Regione Marche (Italy). The authors thank Cristiano Riminesi, from the Institute of Heritage Science, for his invaluable help. This work is dedicated to the memory of Benedetto Mircoli on the occasion of the 120th anniversary of his death.

Conflicts of Interest: The authors declare no conflict of interest.

References

1. Sun, Z.F.; Chang, Y.; Xia, N. Recent Development of Nanomaterials-Based Cytosensors for the Detection of Circulating Tumor Cells. *Biosensors* **2021**, *11*, 281. [[CrossRef](#)] [[PubMed](#)]
2. Davies, S.; Hu, Y.; Jiang, N.; Blyth, J.; Kaminska, M.; Liu, Y.; Yetisen, A.K. Holographic Sensors in Biotechnology. *Adv. Funct. Mater.* **2021**, *31*, 2105645. [[CrossRef](#)]
3. Lucío, M.I.; Cubells-Gómez, A.; Maquieira, Á.; Bañuls, M.J. Hydrogel-based holographic sensors and biosensors: past, present, and future. *Anal. Bioanal. Chem.* **2021**, *414*, 993–1014. [[CrossRef](#)]
4. Castagna, R.; Tombesi, A.; Riminesi, C.; Di Donato, A.; Francescangeli, O.; Lucchetta, D.E. HKUST-1-Doped High-Resolution Volume Holographic Gratings. *Chemosensors* **2022**, *10*, 310. [[CrossRef](#)]
5. Yetisen, A.K. *The Prospects for Holographic Sensors*; Springer International Publishing: Berlin/Heidelberg, Germany, 2015; pp. 149–162.
6. El Joudi, E.M.; Franke, H. Holographic Gratings in Photopolymers as Optical Gas Monitors. In *Applications of Photonic Technology 2: Communications, Sensing, Materials, and Signal Processing*; Lampropoulos, G.A., Lessard, R.A., Eds.; Springer: Boston, MA, USA, 1997; pp. 915–921. [[CrossRef](#)]
7. Vita, F.; Lucchetta, D.E.; Castagna, R.; Criante, L.; Simoni, F. Effects of resin addition on holographic polymer dispersed liquid crystals. *J. Opt. Pure Appl. Opt.* **2009**, *11*, 024021. [[CrossRef](#)]
8. Wongkaew, N.; Simsek, M.; Griesche, C.; Baeumner, A.J. Functional Nanomaterials and Nanostructures Enhancing Electrochemical Biosensors and Lab-on-a-Chip Performances: Recent Progress, Applications, and Future Perspective. *Chem. Rev.* **2019**, *119*, 120–194. [[CrossRef](#)]
9. Naresh, V.; Lee, N. A Review on Biosensors and Recent Development of Nanostructured Materials-Enabled Biosensors. *Sensors* **2021**, *21*, 1109. [[CrossRef](#)]
10. Eichler, H.J.; Orlic, S.; Schulz, R.; Rübner, J. Holographic reflection gratings in azobenzene polymers. *Opt. Lett.* **2001**, *26*, 581–583. [[CrossRef](#)]
11. Tomlin, D.; Natarajan, L.; Tondiglia, V.; Sutherland, R.; Bunning, T. Morphology of Holographic Polymer Dispersed Liquid Crystal Reflection Gratings Written in Thiol-ene and Acrylate Polymer Hosts: Part I-Grating Formation. *Microsc. Microanal.* **2003**, *9*, 382–383. [[CrossRef](#)]
12. Hu, Y.; Kowalski, B.A.; Mavila, S.; Podgórski, M.; Sinha, J.; Sullivan, A.C.; McLeod, R.R.; Bowman, C.N. Holographic Photopolymer Material with High Dynamic Range (Δn) via Thiol–Ene Click Chemistry. *ACS Appl. Mater. Interfaces* **2020**, *12*, 44103–44109. PMID: 32844645. [[CrossRef](#)]
13. Castagna, R.; Lucchetta, D.E.; Rippa, M.; Xu, J.H.; Donato, A.D. Near-frequency photons Y-splitter. *Appl. Mater. Today* **2020**, *19*, 100636. [[CrossRef](#)]
14. Shalit, A.; Lucchetta, D.; Piazza, V.; Simoni, F.; Bizzarri, R.; Castagna, R. Polarization-dependent laser-light structured directionality with polymer composite materials. *Mater. Lett.* **2012**, *81*, 232–234. [[CrossRef](#)]
15. Castagna, R.; Lucchetta, D.E.; Vita, F.; Criante, L.; Simoni, F. At a glance determination of laser light polarization state. *Appl. Phys. Lett.* **2008**, *92*, 041115. [[CrossRef](#)]
16. Bunning, T.J.; Natarajan, L.V.; Tondiglia, V.P.; Sutherland, R.L. Holographic Polymer-Dispersed Liquid Crystals (H-PDLCs). *Annu. Rev. Mater. Sci.* **2000**, *30*, 83–115. [[CrossRef](#)]
17. Castagna, R.; Vita, F.; Lucchetta, D.E.; Criante, L.; Simoni, F. Superior-Performance Polymeric Composite Materials for High-Density Optical Data Storage. *Adv. Mater.* **2009**, *21*, 589–592. [[CrossRef](#)] [[PubMed](#)]
18. Lucchetta, D.; Spegni, P.; Di Donato, A.; Simoni, F.; Castagna, R. Hybrid surface-relief/volume one dimensional holographic gratings. *Opt. Mater.* **2015**, *42*, 366–369. [[CrossRef](#)]
19. Sutherland, R.L.; Natarajan, L.V.; Tondiglia, V.P.; Bunning, T.J. Bragg gratings in an acrylate polymer consisting of periodic polymer-dispersed liquid-crystal planes. *Chem. Mater.* **1993**, *5*, 1533–1538. [[CrossRef](#)]
20. Castagna, R.; Nucara, L.; Simoni, F.; Greci, L.; Rippa, M.; Petti, L.; Lucchetta, D.E. An Unconventional Approach to Photomobile Composite Polymer Films. *Adv. Mater.* **2017**, *29*, 1604800. [[CrossRef](#)]
21. Castagna, R.; Donato, A.D.; Strangi, G.; Lucchetta, D.E. Light controlled bending of a holographic transmission phase grating. *Smart Mater. Struct.* **2022**, *31*, 03LT02. [[CrossRef](#)]
22. Lucchetta, D.; Vita, F.; Francescangeli, D.; Francescangeli, O.; Simoni, F. Optical measurement of flow rate in a microfluidic channel. *Microfluid. Nanofluidics* **2016**, *20*, 1–5. [[CrossRef](#)]
23. Lucchetta, D.; Simoni, F.; Hernandez, R.; Mazzulla, A.; Cipparrone, G. Lasing from chiral doped nematic liquid crystal droplets generated in a microfluidic device. *Mol. Cryst. Liq. Cryst.* **2017**, *649*, 11–19. [[CrossRef](#)]
24. Orlic, S.; Dietz, E.; Frohmann, S.; Mueller, C.; Schoen, R.; Trefzer, M.; Eichler, H.J. High-density multilayer recording of microgratings for optical data storage. In *Proceedings of the Organic Holographic Materials and Applications II*. SPIE, Denver, CO, USA, 2–6 August 2004; Volume 5521, pp. 161–173.
25. McLeod, R.R.; Daiber, A.J.; McDonald, M.E.; Robertson, T.L.; Slagle, T.; Sochava, S.L.; Hesselink, L. Microholographic multilayer optical disk data storage. *Appl. Opt.* **2005**, *44*, 3197–3207. [[CrossRef](#)] [[PubMed](#)]

26. Barachevskii, V.A. Photopolymerizable recording media for threedimensional holographic optical memory. *High. Energy Chem.* **2006**, *40*, 131–141. [[CrossRef](#)]
27. Hesselink, L.; Orlov, S.S.; Bashaw, M.C. Holographic data storage systems. *Proc. IEEE* **2004**, *92*, 1231–1280. [[CrossRef](#)]
28. Blanche, P.A.; Gailly, P.; Habraken, S.L.; Lemaire, P.C.; Jamar, C.A.J. Volume phase holographic gratings: large size and high diffraction efficiency. *Opt. Eng.* **2004**, *43*, 2603–2612. [[CrossRef](#)]
29. Gamboa, J.; Hamidfar, T.; Vonckx, J.; Fouda, M.; Shahriar, S.M. Thick PQ:PMMA transmission holograms for free-space optical communication via wavelength-division multiplexing. *Appl. Opt.* **2021**, *60*, 8851–8857. [[CrossRef](#)]
30. Neipp, C.; Taleb, S.I.; Francés, J.; Fernández, R.; Puerto, D.; Calzado, E.M.; Gallego, S.; Beléndez, A. Analysis of the Imaging Characteristics of Holographic Waveguides Recorded in Photopolymers. *Polymers* **2020**, *12*, 1485. [[CrossRef](#)]
31. Wang, Q.; Lian, M.; Zhu, X.; Chen, X. Excellent humidity sensor based on ultrathin HKUST-1 nanosheets. *RSC Adv.* **2021**, *11*, 192–197. [[CrossRef](#)]
32. Lucchetta, D.E.; Donato, A.D.; Singh, G.; Castagna, R. Lasing in Haloalkanes-based polymeric mixtures. *Opt. Mater.* **2022**, *131*, 112614. [[CrossRef](#)]
33. Lucchetta, D.E.; Castagna, R.; Singh, G.; Riminesi, C.; Di Donato, A. Spectral, Morphological and Dynamical Analysis of a Holographic Grating Recorded in a Photo-Mobile Composite Polymer Mixture. *Nanomaterials* **2021**, *11*, 2925. [[CrossRef](#)]
34. Kogelnik, H. Coupled Wave Theory for Thick Hologram Gratings. *Bell Syst. Tech. J.* **1969**, *48*, 2909–2947. [[CrossRef](#)]
35. Kogelnik, H. Coupled wave theory for thick hologram gratings. In *Landmark Papers on Photorefractive Nonlinear Optics*; World Scientific Publishing: Singapore, 1995; pp. 133–171.
36. Liu, Y.; Fan, F.; Hong, Y.; Zang, J.; Kang, G.; Tan, X. Volume holographic recording in Irgacure 784-doped PMMA photopolymer. *Opt. Express* **2017**, *25*, 20654–20662. [[CrossRef](#)] [[PubMed](#)]
37. Li, Y.; Wang, X.; Sun, J. Layer-by-layer assembly for rapid fabrication of thick polymeric films. *Chem. Soc. Rev.* **2012**, *41*, 5998–6009. [[CrossRef](#)]
38. Ebner, C.; Mitterer, J.; Eigruber, P.; Stieger, S.; Riess, G.; Kern, W. Ultra-High Through-Cure of (Meth)Acrylate Copolymers via Photofrontal Polymerization. *Polymers* **2020**, *12*, 1291. [[CrossRef](#)] [[PubMed](#)]
39. Kolczak, U.; Rist, G.; Dietliker, K.; Wirz, J. Reaction Mechanism of Monoacyl- and Bisacylphosphine Oxide Photoinitiators Studied by ³¹P-, ¹³C-, and ¹H-CIDNP and ESR. *J. Am. Chem. Soc.* **1996**, *118*, 6477–6489. [[CrossRef](#)]
40. Lucchetta, D.; Criante, L.; Simoni, F. Optical characterization of polymer dispersed liquid crystals for holographic recording. *J. Appl. Phys.* **2003**, *93*, 9669–9674. [[CrossRef](#)]
41. Lucchetta, D.; Criante, L.; Simoni, F. Determination of small anisotropy of holographic phase gratings. *Opt. Lett.* **2003**, *28*, 725–727. [[CrossRef](#)]